Experimental Behaviour of Nailed Soil by GFRP Bars

S. Sghaier[1], S. Ellouze[1], M. Bouassida[2], A. Bezuijen[3], B. Hadrich [4] and A. Daoud[1]

[1] *Research unit of Geomaterials, Structures in Civil Engineering and Environment (GESTE), National Engineering school of Sfax (ENIS), University of Sfax, Tunisia*

[2] *Laboratory of Geotechnical Engineering and Georisk, National Engineering School of Tunis (ENIT), University of Tunis El Manar, Tunisia*

[3] *Geotechnics laboratory, Faculty of Engineering and Architecture, Ghent University, Belgium*

[4] *Department of Chemical Engineering, College of Engineering, Imam Mohammad Ibn Saud Islamic University, IMSIU, Riyadh 11432, Saudi Arabia*

E-mail : souhir.ellouze@enis.tn

ABSTRACT: Replacing steel reinforcements with the inclusions of Glass Fiber Reinforced Polymer (GFRP) is one of the most promising solutions not only to overcome corrosion problems, but also to improve soil nail durability as a tool of slopes stabilization and retaining excavations. The present study provides an insightful knowledge regarding the pull-out behaviour of a GFRP nail observed in laboratory from a pull-out test. It is a parametric study, which includes the influence of nail dimensions, the overburden pressure, and the degree of saturation, essentially on the pull-out load of the GFRP nail. Using an experimental working method, based on a full factorial design, the study reveals that the influence of nail dimensions and the overburden pressure on the pull-out load are more significant than that of the degree of saturation. Moreover, the experimental results show that the pull-out behaviour of the GFRP reinforcement is different from the ribbed steel reinforcement, subjected the same testing condition. The differences between the Young's modulus, the interface properties, and the surface roughness of the bar exhibit the main influence factors.

KEYWORDS: GFRP nail, Pullout test, Soil-nail interaction, and Design of experiments methodology.

1. INTRODUCTION

Reinforcement of weak soils by nails has numerous benefits. They are manifested in the potential of increasing the in-situ soil shear strength and of providing better stability. Northern Thailand is a hotspot for landslides. In this region, rainfall-triggering landslides have caused many deaths and sufferings. Avirut *et al.* (2022) proposed a landslide-triggering rainfall threshold for Northern Thailand. It is based on rainfall data of 48 triggering rainfall events, causing 59 landslides in the investigated area. The author divided the threshold into two parts of different duration of rainfall events to account for the mechanisms of landslide formation. Their study constitutes the first suggestion to incorporate these types of mechanisms. The introduced threshold showed positive prediction signs, notably of false alarm rate, false alarm ratio, and a critical success index. It is also useful for landslide warning systems in the study investigated area of Northern Thailand.

On July 28th, 2018, a massive landslide occurred in a mountainous area of the Northern Thailand. After ten days of heavy rains, the landslide generated the movement of an uphill mountain soil into the populated village. A slope stability analysis is performed by Veerayut *et al.* (2021) to assess the landslide hazard, regarding the results of an aerial photogrammetric survey, a field exploration, and a set of laboratory tests. The slope stability analysis and rainfall records revealed that the Huay Khab landslide was mainly caused by an increase in the water content of residual soils due to the prolonged rainfall, which led to a sharp decrease in the shear strength.

Pitchaya *et al.* (2022) investigated the performance of the bioengineering techniques using 3D stability-seepage modelling. The results indicated that the critical locations on slopes, as the lowest factor of safety, are not necessarily stationary. They could change with an ongoing water infiltration and seepage. It is concluded that the bioengineered slope covered with early-stage pioneer plants and rubber trees have a lower stability factor of safety than the natural forest. It implies that the surface slope covered with the early-stage pioneer plants is more likely to fail during heavy rains. These findings highlight the importance of incorporating a 3D stability model for land examination, considering the fact that land coverage can have noticeable influences on slope stability.

Thanh Son *et al.* (2018) studied the effect of root reinforcement on the stability of vegetated slope under rainfall condition. They conducted a transient seepage and slope stability analysis, relying on the finite element as well as the limit equilibrium methods. A field monitored on a residual soil slope is numerically modelled for the region of Thailand. The results showed that the contribution of root cohesion on slope stability is much more significant for the non-compacted soil condition than that of the well-compacted one. Moreover, it is found that both modelled and monitored pore-water pressure reach the highest values about one day, after the peak of a daily rainfall. Thanh Son *et al.* (2018) concluded that this finding has a significant implication on rainfall-based landslide warning.

Thanh *et al.* (2017) suggested probabilistic analyses for assessing the stability of unsaturated soil slope subject to a rainfall. They conducted a series of seepage and stability analyses of an infinite slope based on random fields for the purpose of studying the influence of the spatial variability of shear strength parameters on the probability of rainfall-induced slope failure. Their results corroborate that a probabilistic analysis is efficient for qualifying various locations of the failure surface caused by the spatial variability of soil shear strength for a shallow infinite slope failure due to rainfall.

Thanh *et al.* (2018) introduced a probabilistic framework for slope stability analysis considering the spatial variability of root reinforcement. A residual soil slope under a heavy rainfall event is used to model the seepage and stability analysis. They carried out a probabilistic analysis considering both stationary and non-stationary random fields of root cohesion. The results disclosed that the failure of the vegetated slope could occur when the variance coefficient of the root cohesion is greater than the critical value. Thanh et al. 2018 came to the conclusion that in practice, the efficiency of the bioengineering method can be improved by controlling the variation of root cohesion within such limitations.

Passive soil nailing has been widely adopted, as an effective, reliable and versatile technique over the last two decades. It is currently the predominant method used not only to upgrade the stability of man-made and natural slopes but also to prevent excessive displacements (Kanoun *et al.,* 2017).

Since 1970, under the Landslip Preventive Measures program launched by the Geotechnical Engineering Office of Hong Kong,

nailed slopes have gained extensive practice (Cheng *et al.,* 2009). The basic concept of soil nailing involves the placement of a steel bar into a pre-drilled hole. The remaining space is filled with a cement grout, which is mainly used to transfer tensile stresses, generated in the inclusions, into the soil mass through the mobilization of friction at the soil-nail interface. Essentially, it protects the steel bar from a direct exposure to moist soil mass. However, micro cracks will occur due to the tensile stresses transmitted to the cement grout. In this case, the steel surface will be attacked by water, chemicals, and other corrosion promoting agents through micro-cracks (Shiu *et al.,* 2003), leading to a reduction of the steel bar strength. The corrosion of steel bars is mainly revealed by a set of experiences as the main cause of deterioration (Shiu and Cheung, 2014; Chen *et al.,* 2015). Despite the adoption of extra protection measures aiming to prevent the corrosion of steel, notably a double corrosion system and galvanized zinc coating, which is accompanied by a 2mm sacrificial steel thickness (Koor and Cheung, 2005; Cheng *et al.,* 2016). The long-term effectiveness of steel nails, installed in aggressive environments, cannot be guaranteed. Currently, many researchers have been focusing on investigating the performance of innovative materials, which replace steel reinforcement and enhance the durability of nails. Glass Fiber Reinforced Polymer has drawn the specialists' attention in recent years, regarding its typical benefits over steel such as higher strength to weight ratio, better corrosion resistance, and easier site handling (Cheng *et al.,* 2009; Zhang *et al.,* 2014; Xu *et al.,* 2017; Chen *et al.,* 2020).

However, to adopt these new composite materials in geotechnical engineering the features above mentioned are not sufficient. A strong bond between the soil and the inclusion is required. Installed nails in the passive zone are subject to a pull-out force resulting from the slope movement. It seems that the pull-out capacity developed at the soil-nail interface is a critical parameter for the soil-nail design. Furthermore, the soil-nail interface behaviour depends on the factors: overburden pressure, surface roughness, nail dimensions and the degree of saturation of soil (Lee *et al.,* 2001; Hong *et al.,* 2003; Junaideen *et al.,* 2004; Pradhan *et al.,* 2006; Su *et al.,* 2008, Samanta *et al.,* 2018).

To date, the strengthening of concrete structures, using fiber reinforced Polymers, has trendily been used to improve structural performances, particularly an increase in strength and stiffness of the structural members (Tidarut *et al.,* 2019, Tidarut *et al.,* 2020, Tidarut *et al.,* 2021). Tidarut *et al.,* 2019 conducted a series of uniaxial compression tests on confined concrete cylinders by cotton, jute, and hemp natural fibre reinforced polymer (NFRP). The results proved that the NFRP is effective and suitable for enhancing the confinement effect of concrete, notably Jute-NFRP.

Tidarut *et al.* (2020) examined the use of a natural jute fabric reinforced polymer (JFRP) composite sheets as an external strengthening material of reinforced concrete (RC) beams. They investigate the shear behaviour of pre-damaged RC beams strengthened with JFRP sheets, which is subjected to non-reversed cyclic three-point bending load test. The results display that the JFRP improve the shear strength of tested beams significantly. The shear enhancement of JFRP strengthened pre-damaged beams are compared to that of non-damaged beams strengthened by conventional FRPs. They proved the applicability of the strengthened JFRP in pre-damaged shear-deficient beams.

Tidarut *et al.* (2021) carried out a series of compression tests on water hyacinth fibre-reinforced polymer composite confined concrete to investigate the improved strength and ductility performance. They found that the mechanical properties of water hyacinth fibre-reinforced polymer composite, such as tensile strength (137 MPa) and ultimate tensile strain (1.72%), are acceptable for concrete strengthening purposes. Importantly, in comparison with the conventional fibre reinforced polymer composites, the use of water hyacinth fibre-reinforced polymer composite is rewarded by its environmental friendliness.

Besides, Tidarut *et al.* (2021) put into practice a series of compression tests on plastic straw fibre-reinforced polymer composite (PSFRP) confined concrete. They investigated their improved strength and ductility performance. The results revealed that the compressive strength enhancement is increased, ranging from 2.41% to 28.37%. The PSFRP confinement contributes to a larger strengthening effect for the low strength concrete of PSFRP, indicating a suitable performance of the PSFRP for concrete strengthening purposes.

Linh Van *et al.* (2022) investigated the bond behaviour between the embedded through-section fiber-reinforced polymer (ETS FRP) bars and concrete, by carrying out pull-out tests, and complementing a simple nonlinear finite element (FE) analysis. A parametric study was conducted to look for the effects of some key features, such as the properties of adhesives, FRP bars, and concrete, on the bond performance of the ETS FRP bar–concrete interfaces. Based on the parametric study, they formulated expressions for the maximum bond force and the effective bond length.

For soil reinforcement, many researchers investigated the influence of some key factors on the pull-out capacity of GFRP nails. Sharma *et al.* (2019) examined the influence of the overburden pressure, the relative density and the surface roughness on the pull-out behaviour of grout-free steel nails. They noticed that an increase in the normalized roughness causes an increase of more than twofold the maximum pull-out resistance, under an overburden pressure range of 7.75-99 kPa. In addition, Sharma *et al.,* 2020 examined the effect of surface roughness on the interface shear behaviour between the grout-free steel nail and dry medium sand through a series of pull-out and direct shear tests. They end with the fact that the surface roughness is considered as a key parameter governing the interface shear stress of the steel nail.

Yeung *et al.* (2007) investigated the pull-out performance of GFRP pipe by carrying out field pull-out tests. They found that the combination of GFRP pipe with the pressure grouting has the potential to replace steel nails. Zhu *et al.* (2011) evaluated the performance of the same system during two field pull-out tests. They proved that this system possesses a satisfactory efficiency, and the double grouting method could improve the pull-out capacity of GFRP nail. Pei *et al.* (2013) utilized Fiber Bragg Grating (FBG) to investigate the performance of GFRP nail during a laboratory pull-out test. They pointed out that the pull-out behaviour of this new composite material is similar to that of a cement grouted steel nail.

Zhang *et al.* (2014) performed a set of pull-out tests on GFRP bars and strip under low normal stress. They found that, in comparison to steel reinforcement, GFRP material has a more non-linear and non-uniform distribution of the interface shear stress. Additionally, the pull-out behaviour is more progressive. Zhang *et al.* (2015) studied the time-dependent interaction mechanism between GFRP nail and sand during laboratory pull-out test. They noted that the tensile forces and the shear stresses at the soil-nail interface are time dependent.

Chen *et al.* (2015) conducted a research on the long-term performance of the GFRP reinforcement. A field pull-out test is carried out on a GFRP nail buried in a slope during three years, using the technology of sensing Fiber Bragg grating (FBG). Based on the monitoring results, they confirmed that this material is durable and able to enhance the stability of slopes. Chen *et al.* (2020) scrutinized the influence of different mortar constraint conditions on the pull-out behaviour of GFRP nails. They found that the ultimate tensile stress at GFRP nail-mortar interface exceeds the tensile strength of conventional steel nails, indicating that these materials can be an alternative to steel nails.

In this respect, it is concluded that the GFRP material can be a competitive solution to replace steel material, owing to its high corrosion resistance, lightweight, high stiffness and adaptability to sensors. It is worth noting that the pull-out behaviour of GFRP nails is quite different from the steel nails one. Accordingly, there is a need to understand the interactive mechanism between the GFRP nail and the soil to adopt this new composite material in geotechnical applications. The main goals of this paper are the comparison of the pull-out performance of grout-free GFRP and steel nails buried in a sand. Furthermore, this study sets out to

examine the effect of some key factors on the GFRP nail pull-out load and to determine the optimum conditions leading to a maximum pull-out resistance. The originality of this study relies first in the characterization of the pull-out performance of the GFRP nail, compared to the conventional steel nail subjected to the same conditions. Secondly, the use of the "design of experiments methodology", helps to examine the effect of the parameters governing the bond strength between the nails and the soil. The adoption of this methodology serves to achieve the main objectives of this study with the minimum experiments and hence costs. Moreover, it is rarely used in geotechnical engineering applications.

By performing a laboratory pull-out setup, the implementation of nail pull-out tests with a controlled displacement rate, involved four main factors: nail diameter, embedded length of nail, overburden pressure, and the degree of saturation of the soil. A full factorial design is considered in this study. The chosen k factor is set at two different levels. The creation of a 2k factorial design is helpful for the evaluation of responding at all the combinations of the k factors and levels.

2. PROBLEM STATEMENT

The long-term performance of nailed soil structures requires the ability of nails to withstand corrosive attacks from its local environment. Cement grout can serve to protect the nails from corrosion by forming physical and chemical barriers. Physically, the grout separates the steel bar from the surrounding soil. The alkalinity of the grout provides the chemical protection function, which leads to the formation of a tight oxide film on the steel surface. One notes that when the steel bar is loaded, the cement grout exhibits tensile stresses. As such, micro-cracks will occur and break the chemical barrier allowing oxygen, water and other corrosion promoting agents to be in contact with the steel bar. To overcome this problem, GFRP materials are a potentially suitable alternative to substitute steel. They eliminate most of the durability concerns. However, some questions are posed by the potential users of these composite materials. As the mechanical and physical properties of GFRP nails are different from those of steel nails, the bond strength and the failure mode require an investigation. In fact, the basic design of the soil nail system consists of transferring the tensile stresses generated within the reinforcement to the surrounding soil by the mobilized friction at the soil-nail interface. It appears that, the pull-out capacity is a key design factor for a proper analysis of the reinforced structure. This kind of parameter is the most important indicator of the soil nail performance. Nailed soils are among the viable solutions to stabilize the geotechnical structures wherein the pull-out failure is necessarily taken into consideration. This paper essentially suggests an experimental design methodology for studying the bond strength and the failure mechanism of GFRP nails in a non-grouted situation. In these veins, the pull-out performance of these new composite materials in geotechnical engineering is investigated and the effect of some key factors on the pull-out capacity is examined.

3. MATERIALS AND METHODOLOGY

3.1 Material Properties

3.1.1 Sand

A series of laboratory tests are carried out to determine the basic parameters of the selected sand used to perform the laboratory experiments. The testing procedures are pursued as it is stipulated in the relevant clauses of the American Society for Testing and Materials (ASTM). The relevant geotechnical parameters of the tested sand are summarized in Table 1.

The particle size distribution of the sand was determined by the dry sieving method. The grain size curve of the tested sand is displayed in Figure 1. According to the Unified Soil Classification System, the tested sand sample is a poorly graded fine sand (SP).

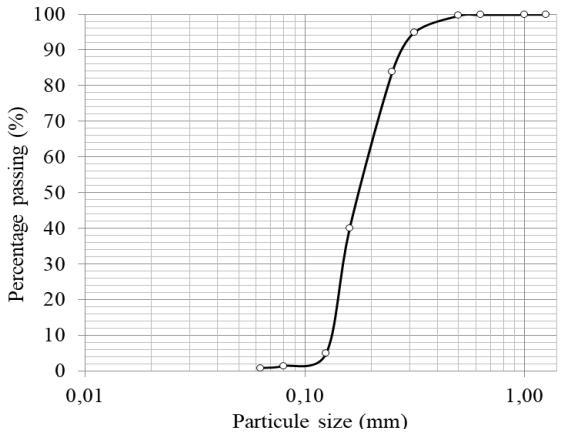

Figure 1 Grain size distribution of the tested sand

Standard direct shear tests, under normal stresses ranging from 25 to 200 kPa, were carried out to determine the shear strength parameters of the sand. The test is repeated three times. Figure 2 shows the variation of the average peak shear stresses versus the applied normal stresses. The soil drained friction angle estimated from the test results is 31°.

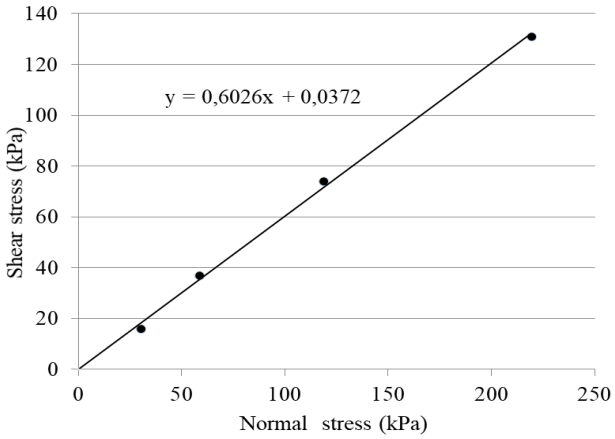

Figure 2 Variation of the peak shear stress versus normal stress from the direct shear test

Table 1 Physical and mechanical properties of the sand

Properties	Unit	Value
Specific gravity (G_s)	____	2.65
Average grain size (D_{50})	mm	0.18
Coefficient of uniformity (C_u)	____	1.41
Coefficient of curvature (C_c)	____	0.93
Maximum dry unit weight (γ_{dmax})	(kN/m^3)	17.27
Minimum dry unit weight (γ_{dmin})	(kN/m^3)	15.02
Drained friction angle (φ')	°	31

The pycnometer test was carried out within the standard of the ASTM D854-00 to measure the specific gravity of the test sand. Minimum (γ_{dmin}) and maximum (γ_{dmax}) dry unit weights of the sand specimen have been determined.

3.1.2 GFRP Material

The used nails in this study consists of GFRP bars made of glass fibers embedded in a resin matrix with different diameters and lengths fabricated through the pultrusion process by Composite Building Innovation (a Tunisian factory) as shown in Figure 3. Steel bars of diameter 10 mm and of length 0.40 m are also tested for the purpose of comparison.

Figure 3 GFRP nails of different diameters

The typical properties of steel and GFRP reinforcements are presented in Table 2. The GFRP nails have a higher axial tensile strength than the steel ones. However, the GFRP Young modulus is lower roughly by one fourth, compared to the one of steel bars. In addition, the GFRP material, with a density equals 28% is lighter than steel. It renders the transportation, handling, and installation of GFRP nails much easier, particularly for the slope stabilization projects. For this reason, the GFRP bars are considered as an appropriate alternative to the steel reinforcements.

Table 2 Physical and mechanical properties of Steel and GFRP nails

Material	Density ρ (kg/m^3)	Young modulus (GPa)	Ultimate tensile strength (MPa)	Strain at Ultimate Limit State (%)	Rib area f_R of nominal diameter 10 mm
Steel	7800	210	400	0.2	0.076
GFRP	2200	> 50	> 1000	2.0	0.035

The surface roughness of steel and the GFRP inclusions are characterized by the profile maximum height, calculated as the distance between the highest peak and the deepest valley on the bar surface. Each reinforcement, height and spacing are measured while the related rib area is calculated from Equation (1) (Makni *et al.,* 2014).

$$f_R = A_n \sin\beta / (\pi D s) \quad (1)$$

f_R corresponds to the related rib area; A_n is the area of the rib; β is the angle between the rib and the longitudinal axis of the nail; s corresponds to the spacing between the ribs, and D is the external diameter of the bar.

3.2 Experimental Procedures

The pull-out tests were performed by using a laboratory pull-out test box with the internal dimensions of 950 mm length, 580 mm wide and 565 mm high. The test box is composed of six steel plates fixed together. Bolted connections are used (Figures 4 and 5). This test box enables carrying out the pull-out test with a controlled displacement-rate. This experiment describes the pull-out response of a GFRP nail from the elastic behaviour up to failure. The nail is pulled out by means of a manual hydraulic pump equipped with a cylinder of hollow piston. Upon action on the pump lever, the fitted piston in the cylinder is withdrawn, resulting in the pull-out of the nail. The nail is connected to a force sensor fixed to a reaction frame, to measure the pull-out force. The displacement of the nail is measured by two linear variable differential transducers (LVDTs) fixed to the GFRP nail once it is pulled out horizontally.

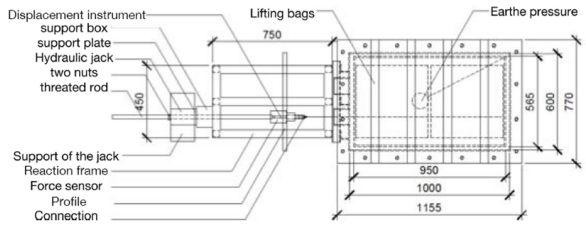

(a) Plan

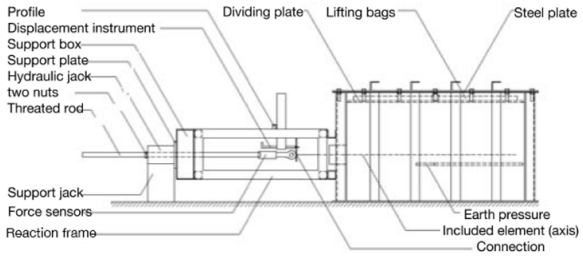

(b) Side view

Figure 4 Sketch of the experimental device

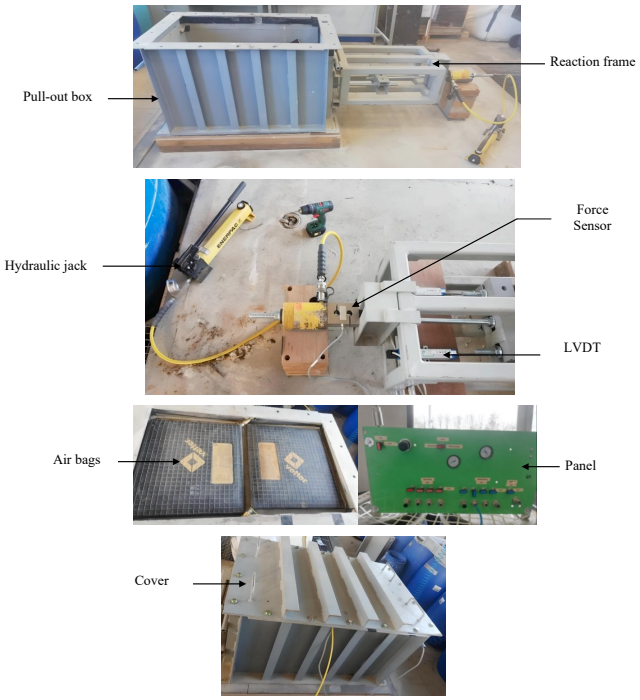

Figure 5 Pullout test set-up

The soil sample is prepared, in a dense medium state, for the laboratory pull-out tests. Since the uniformity of soil can highly influence the pressure distribution on the nails, the soil sample is required to have a uniform density. In this light, the box is filled with sub-layers of 10 cm thickness; the soil mass weight is known. The soil mass of each layer is required to achieve the targeted relative density (RD) of 68%, which is weighed and poured into the box. Hence, the compacted sand is levelled up to the targeted elevation by using a vibrating plate. The desired density is achieved by checking the level of the lines drawn on the inner faces of the box wall. When the compacted sand reached 250 mm of height of the pull-out box, the GFRP nail is placed by hand and aligned smoothly. This method of installation is different from the classical grouting installation. However, it provides the frictional resistance

between the compacted sand and the applied pressure on the surface of the experimental model. Later, the following compacted sand layers continue up to the final height of 65 mm at the top of compacted sand where a plate and air bags are placed. Once the pull-out box is full, the required overburden pressure is applied by using two mini air bags placed under the cover, and the whole surface of the sampled sand is filled, as shown in Figure 5. The applied pressure is controlled by a panel during the experiment. The force sensor and the linear variable differential transducers are connected to a computer for an automatic data acquisition.

3.3 Experimental Program

The proper design of a nailed soil system requires an understanding of the interactive mechanism between the nails and the soil. At the soil-nail interface, bond resistance is developed by a relative displacement between the nail and the soil. This resistance is investigated by performing pull-out tests. Furthermore, the GFRP nailed soil interaction is influenced by a number of factors among which are the nail's diameter, the embedded length, the overburden pressure, and the degree of soil saturation. Hence, to understand the interactive mechanism of the GFRP nails and to evaluate the effect of the above factors on the pull-out load, running pull-out tests is required.

3.3.1 Experimental Design Methodology

The experimental design method is useful for studying the sets of the named physical, mechanical, and chemical phenomenal evolution, depending on a certain number of factors. Traditionally, scientists do sequential experiments in order to examine the effects of the specific variable on the selected response, or else, to find out the optimal conditions, leading to the desired response. This method consists of varying each factor over its range by keeping all the other variables fixed. This methodology gives some results without the interactions between all the required factors. Equally, sometimes it leads to numerous unnecessary runs. In this respect, this methodology isn't an efficient and economic strategy.

The experimental design methodology seems to be the best alternative to any kind of traditional analysis. Its basics lie in varying multiple factors at the same time, instead of one factor at a separated time. This experimental design may enable the experimenter to identify the effect of each factor on the response. It also determines whether the factors interact together or not. Furthermore, it helps to identify the best factorial combination so as to achieve an optimized response. (Myers *et al.,* 2002; Correia *et al.,* 2010; Mukharjee *et al.,* 2014).

3.3.2 Full Factorial Design of Experiments

For the factorial design of experiments, four factors are chosen: the nail diameter (D), the embedded length (L) of the nail, the overburden pressure (P), and the degree of soil saturation (S_r). Each factor is run at two levels selected as follows: 10 and 18 mm, 40 and 60 cm, 50 and 150 kPa and 24 and 72 %, respectively as shown in Table 3. The coded values of the different tested factors are indicated by '-1' for the lowest level and '+1' for the highest level. For example, the lowest level of the nail diameter factor is 10 mm corresponding to '-1' and its highest level is 18 mm corresponding to '+1'. Sixteen experimental runs were performed under different conditions, following the experimental design requirements. Each combination is implemented once. Three runs of the centre points of the experimental field are added. The three replicates of the centre points are used to test the linearity of the response. STATISTICA 12.0 software is used to determine the geometrical and the coded notations. Similarly, it randomizes the treatment of the combinations, resulting in a standard and an experimental order. The chosen model response is the pull-out force of the GFRP nail.

Throughout the experimental study, the pullout force is considered as the response variable. The prediction model derived from the experimental design is described by Equation 2. The model fitting process takes solely the 2-factor interactions into account.

$$F = a_0 + a_1 D + a_2 L + a_3 P + a_4 S_r + a_{12} DL + a_{13} DP + a_{14} PS_r + a_{23} LP + a_{24} LS_r + a_{34} PS_r \quad (2)$$

Table 3 Coded values for factors' levels

Factor	Coded factor	Coded level of variable	
Nail diameter (mm)	D	10	18
Embedded length (cm)	L	40	60
Overburden pressure (kPa)	P	50	150
Degree of saturation (%)	S_r	24	72

4. RESULTS AND DISCUSSIONS

4.1 Comparison of Pull-out Performance of GFRP and Steel Nails

For comparative purposes, the pull-out tests were performed on the GFRP and the ribbed steel nails with a diameter of 10 mm, an embedded length of 0.40 m, under an overburden pressure of 50 kPa and at 72% degree of saturation. The variation of the obtained pull out force versus displacement for the two types of nails is drawing in Figure 6. By comparing the pull-out behaviour of these nails, some differences are noted. For instance, Figure 6 shows the pull-out load of the ribbed steel nail is higher than that of the GFRP nail by 50% under the same conditions. Furthermore, the load–displacement curve of the steel nail has a peak value followed by a sharp decrease in the pull-out force up to a residual value. However, no important variation in the pull-out load is observed during the post peak stage for the GFRP inclusion.

The difference in the pull-out behaviour of these two types of nails is probably attributed to a difference in the interlocking of the sand particles, the mobilization of friction at the soil-nail interface, and the passive resistance against the ribs. With reference to Table 2, the related rib area of steel nail is 0.076; whereas it is 0.035 for the GFRP nail. It explains the generation of a higher pull-out resistance of the ribbed steel nail, compared to the GFRP nail. In this respect, the surface roughness has a significant influence on the pull-out resistance of the nailed soil.

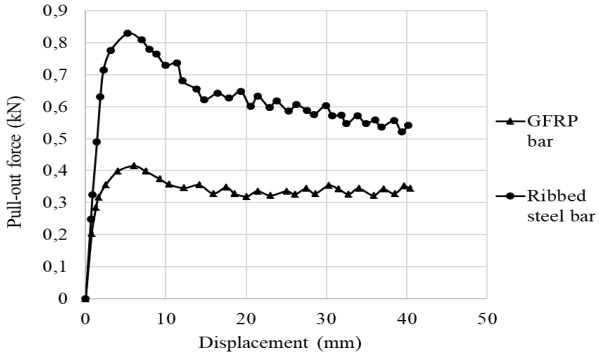

Figure 6 Load-displacement curves recorded from pull-out tests

In order to determine the failure parameters of these two nail types, pull-out tests on the GFRP and the ribbed steel bars were carried out under three different overburden pressures: 50, 100 and 150 kPa at 72% degree of saturation. The variations of the peak shear stress, in function of the applied overburden pressure for the two tested nails, are shown in Figure 7. The test results show that the peak shear stress increases linearly with the overburden pressure. Accordingly, it can be deduced that the pull-out resistance complies with the Mohr Coulomb failure criterion in the investigated pressure range. The equation proposed by Potyondy (1961), which was based on the

Mohr Coulomb yield criterion, is used to evaluate the interface shear strength parameters.

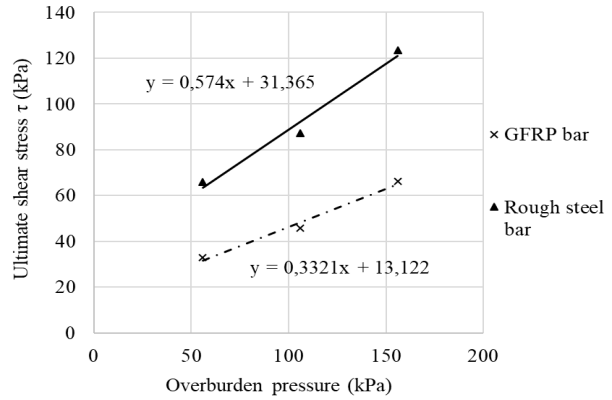

(a)

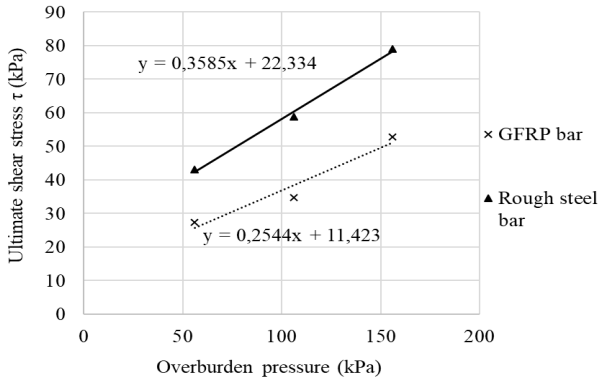

(b)

Figure 7 Recorded peak (a) and residual (b) shear stresses versus the applied overburden pressures

The peak and the residual interface friction angles, mobilized at the soil-nail interface for the two types of nails, are summarized in Table 4.

Table 4 Peak interface friction angles and interface efficiency ratios of tested soil nail interfaces

	Peak		Residual	
Nail type	**Peak interface friction angles δ" (°)**	**Interface efficiency ratios f_δ**	**Residual interface friction angles δ" (°)**	**Interface efficiency ratios f_δ**
GFRP bar	18.37	0.6	14.27	0.46
Ribbed steel bar	29.85	0.96	19.72	0.64

With regard to these results, it is observed that the peak interface friction angle is significantly influenced by the soil-nail surface roughness. Indeed, the peak interface friction angle of the ribbed steel nail remains higher than that of the GFRP nail. It is noted that the friction angle is nearly equal to the peak friction angle of the sand. This result shows that the shear failure zone may move from the soil-nail interface into the soil-soil fine sand in the case of a high surface roughness. The interface efficiency ratio $f_\delta = \delta"/\Phi'$ (i.e., the ratio of interface friction angle to the soil friction angle) of the ribbed steel nail is close to 1. This indicates that the maximum shear stress gets mobilized at the soil-soil interface and that the surface roughness plays an important role in the mobilization of interface friction.

4.2 Load-displacement Curves

The different combinations of the nineteen experiments specified by the 2^4 full factorial design and the corresponding measured values of the ultimate pull-out force of the GFRP nail are presented in Table 5. All the experiments were carried out once. The results of the variation of the pull-out force versus the displacement for experiments N°8, 12, 14, 15 and 16 drawn in Figure 8 using the data of Table 5.

Table 5 Established experiments as per the 2^4 factorial design and the measured values of the pull-out load

Exp. Nb	D	L	P	S_r	w (%)	F (kN)	τ (kPa)
1	10	40	50	24	5.2	0.490	39.027
2	18	40	50			0.754	33.331
3	10	60	50			0.670	35.528
4	18	60	50			1.178	34.713
5	10	40	150			0.887	70.617
6	18	40	150			1.671	73.881
7	10	60	150			1.311	69.527
8	18	60	150			2.415	71.186
9	10	40	50	72	15.7	0.415	33.057
10	18	40	50			0.696	30.752
11	10	60	50			0.635	33.670
12	18	60	50			1.065	31.375
13	10	40	150			0.833	66.271
14	18	40	150			1.511	66.784
15	10	60	150			1.227	65.100
16	18	60	150			2.213	65.227
17	14	50	100	48	10.4	1.030	46.797
18	14	50	100			1.100	49.927
19	14	50	100			1.230	55.800

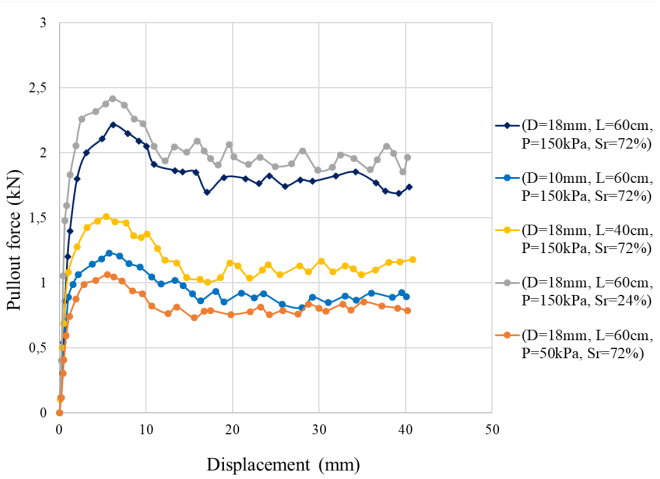

Figure 8 Pull-out load-displacement curves

The pull-out softening behaviour of the tested nail diameters, the embedded length, the overburden pressure and the degree of saturation are shown in Figure 8. From this figure, the load-displacement curves have a distinct peak value followed by a decrease in the pull-out force. This latter increases quasi-linearly up to the peak value. Then, it decreases gradually up to the residual strength, from 6-8 mm displacement. The pull-out softening behaviour corresponds to the results reported by Sharma *et al.*

(2019) for steel nail installed in cohesionless medium soil as well as Sharma *et al.* (2020) for a steel nail installed in a dry medium sand. The increase in the pull-out force can be explained by the high normal stress between the nail and the surrounding soil. It is caused by the restrained dilatancy phenomenon. The decrease in the pull-out force at large displacements refers to the decrease in the normal stress acting on the nail. Indeed, in the post-peak phase, the soil around the nail comes to failure. Due to the conducted pull-out tests at controlled displacement-rate, further displacement of the nail permits a rearrangement of the collapsed soil particles by relative movements. This phase will develop an "arching effect" that induces a decrease in the normal stress around the nail.

4.3 Pull-out Failure Mode

The pictures of Figure 9 were taken after the pull-out tests. They schematize the failure mode and the involved parameters, which affect the pull-out force of the GFRP nail.

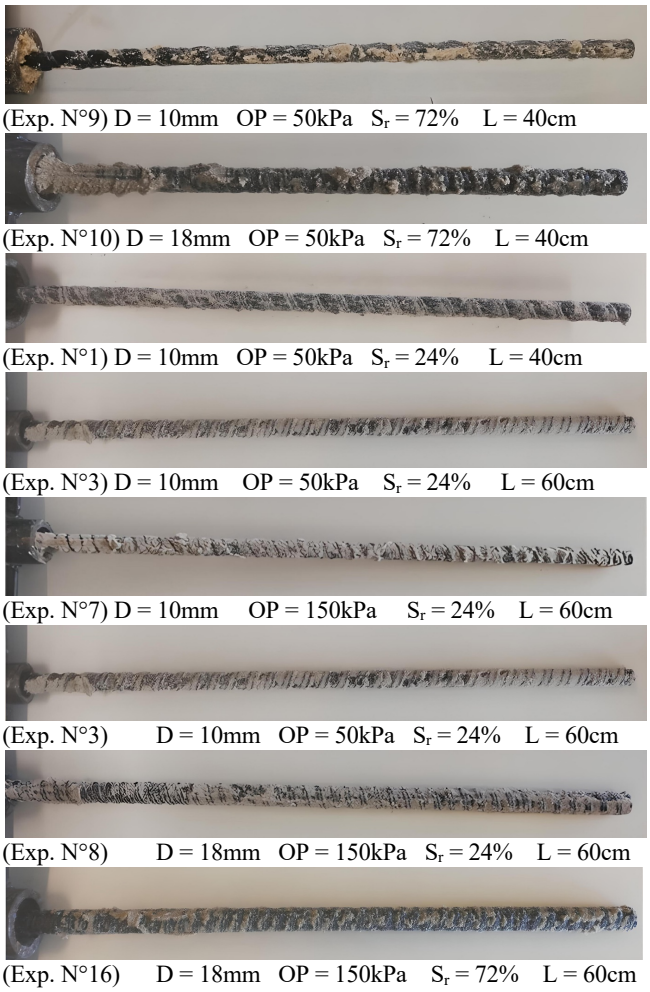

(Exp. N°9) D = 10mm OP = 50kPa S_r = 72% L = 40cm

(Exp. N°10) D = 18mm OP = 50kPa S_r = 72% L = 40cm

(Exp. N°1) D = 10mm OP = 50kPa S_r = 24% L = 40cm

(Exp. N°3) D = 10mm OP = 50kPa S_r = 24% L = 60cm

(Exp. N°7) D = 10mm OP = 150kPa S_r = 24% L = 60cm

(Exp. N°3) D = 10mm OP = 50kPa S_r = 24% L = 60cm

(Exp. N°8) D = 18mm OP = 150kPa S_r = 24% L = 60cm

(Exp. N°16) D = 18mm OP = 150kPa S_r = 72% L = 60cm

Figure 9 Observed failure zones of GFRP nail laboratory tests

The observation following the experiments proves that the failure mode of the GFRP nail is controlled by all the presumed factors related to the nail diameter, the embedded length, the overburden pressure, and the degree of saturation. Figure 9 shows the adhesion of a quantity of soil to the nail surface after the pull-out. Furthermore, an increase in the nail diameter, the embedded length, and the overburden pressure leads to a rise in the soil as shown in pictures Figure 9 (a) and Figure 9 (b), Figure 9 (c) and Figure 9 (d), and Figure 9 (e) and Figure 9 (f), respectively. However, an increase in the degree of soil saturation results in a decrease of the amount of soil between the nail ribs as shown in pictures Figure 9 (j) and Figure 9 (h). This opposite relation gives evidence that the bond strength between the soil and the nail depends almost on all the tested factors.

4.4 Pull-out Resistance of GFRP Nail

In the following sections, an average peak shear stress (τ) is used to examine the effect of the overburden pressure and the degree of soil saturation on the pull-out resistance of the GFRP nail. τ is calculated by referring to the measured peak pull-out force F (kN), which is divided by the active area of the nail A (m^2) from Equation (3).

$$\tau = F/A = F / (\pi DL) \quad (3)$$

The active nail area A is calculated by multiplying the embedded length L (m) of the nail in accordance with the surrounding soil, with the perimeter of the nail πD (m). The test results are summarized in Table 5.

Various theoretical and empirical methods have been proposed to evaluate the peak shear stress that is considered as an important parameter in the design of the soil-nail system. Various forms of soil-nail pull-out models are available. Their original models are referenced by the generic Equation (4) of the Coulomb failure criterion:

$$\tau = c' + \sigma \tan \Phi' \quad (4)$$

c' = effective (drained) cohesion; σ = the normal stress acting on the nail; Φ'= drained internal friction angle.

Potyondy (1961) examined the interface friction between various types of soils (sand, clay and cohesive granular soil) and construction materials (steel, wood and grout). The test results showed that in each case, the grain size distribution, the water content, and the interface roughness have a great impact on the interface friction parameters of the existing material.

In a similar form, Potyondy expressed the interface parameters using Equations (5), (6) and (7):

$$\tau = c_a' + \sigma \tan \delta'' \quad (5)$$

$$c_a' = f_c\, c' \quad (6)$$

$$\tan \delta'' = f_\Phi \tan \Phi' \quad (7)$$

Where: c_a' = apparent cohesion; δ'' = interface friction angle; f_c = coefficient of adhesion; f_Φ = coefficient of friction.

Combining Equations (5), (6) and (7) the interface resistance is related to the soil shear strength parameters. Potyondy's shear stress transfer model is calculated from Equation (8):

$$\tau = f_c\, c' + \sigma f_\Phi \tan (\Phi') \quad (8)$$

In this study, Equation 8 is used to fit the pull-out strength data for obtaining the interface shear strength parameters (c_a', δ'').

4.5 Assessment of the Friction Law of the Interface between the GFRP and the Sand

The assessment of the friction law of the GFRP-sand interface (shear stress τ versus the normal stress acting on the nail σ (Equation 5) is necessary to represent the variation of the pull-out force versus the relative area RA.

The relative area is calculated by referring to the used active area of the nail, which is divided by a reference active nail area from Equation (9).

$$RA = \pi D_i L_i / \pi D_1 L_1 \quad (9)$$

i corresponds to experiments N°1, 2, 3 and 4 for P = 50 kPa and experiments N°5, 6, 7 and 8 for P =150 kPa, as listed in Table 5. The reference active area corresponds to experiment N°1.

The variation of the pull-out force versus the relative area for the first eight tests is represented in Figure 10. It is worth noting that the variation of the pull-out force is linear with the relative area as shown Equation (5), which validates Figure 7.

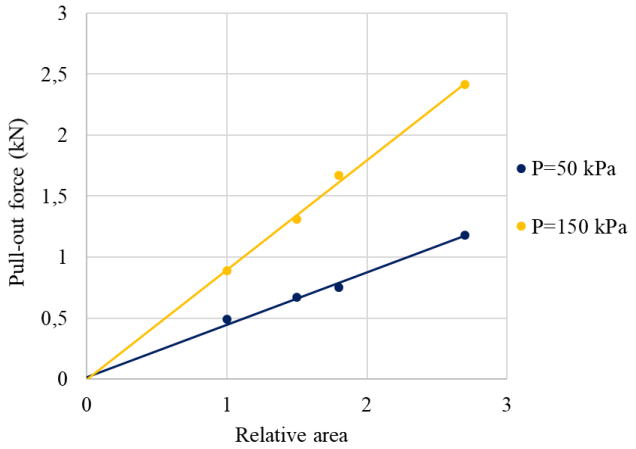

Figure 10 Variation of the pull-out force versus the relative area

4.6 Effects of the Tested Factors on the Pull-out Force of the GFRP Nail

The effects of the nail diameter, the embedded length, the overburden pressure, and the degree of soil saturation on the pullout force of the GFRP nail are shown in Figures 11a, 11b, 11c and 11d. Referring to Figures 11a and 11b, the increase in the nail diameter from 10mm to 18mm and the embedded length from 40cm to 60cm leads to an increase of in the pull-out force of the nail from 0.809 kN to 1.438 kN, and from 0.907 kN to 1.339 kN, respectively. It may be deduced that the more are of the nail diameter and the embedded length of the bar; the more is the contact area between the bar and the soil. This implies that when the area of the interaction between the inclusion and the soil increases, the pull-out force becomes higher.

Furthermore, the increase in the overburden pressure from 50 kPa to 150 kPa results in an increase of the pull-out force of the nail from 0.738 kN to 1.509 kN. Figure 11c illustrates this result. Indeed, a shear zone is created during the nail pull-out in the vicinity of the inclusion. The soil in this zone, although subject to an intense shearing, is constrained against dilatancy by the surrounding soil. This generates an additional local normal stress acting on the nail area. It leads to an increase of the nail pull-out force. In turn, Figure 11d shows that an increase in the degree of saturation of the soil from 24% to 72% leads to a decrease of the pull-out force of the nail from 1.172 kN to 1.074 kN. It is probably attributed to the fact that, at higher water contents, the soil particles possess more water on their surfaces. The adhesion is weaker at the soil-nail interface since the high-water contents give the soil particles more mobility characteristics and the water can be considered as a lubricator between the particles. Thus, low values of pull-out force are mobilized.

The results of the carried-out experiments are invested in the factorial matrix and the software is mainly used to diagnose and model the response surfaces of the pull-out force F. Factors effects (or interaction) with significance level of 5% or lower are considered statistically significant.

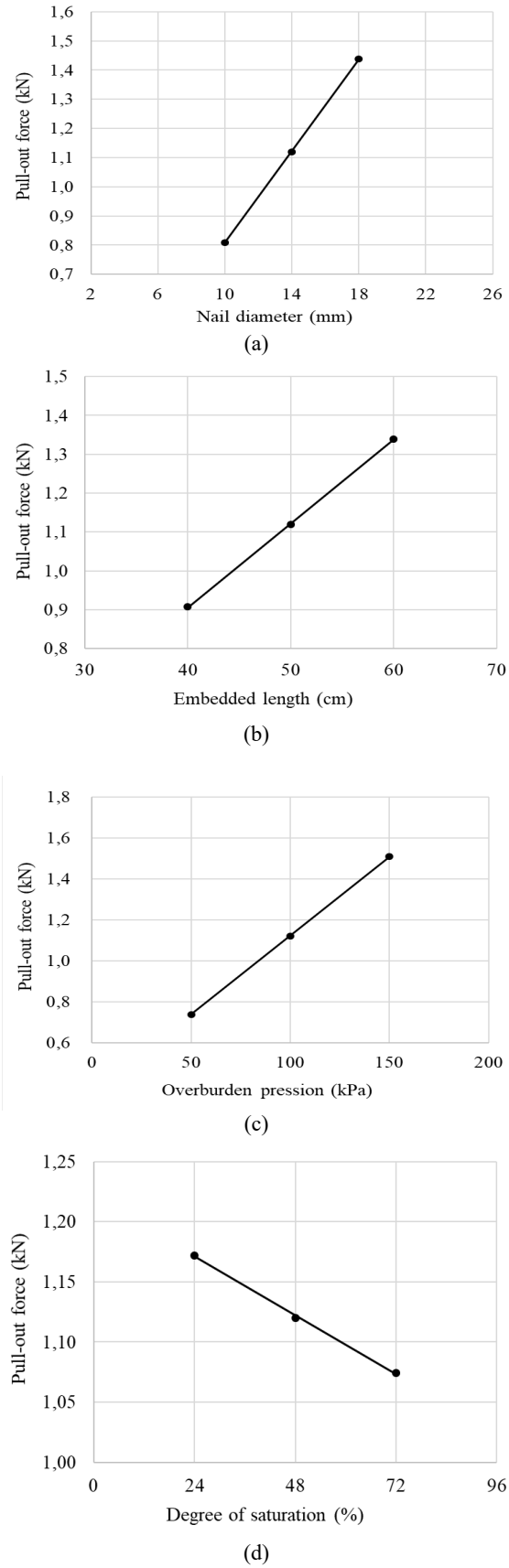

Figure 11 Main effects of nail diameter, embedded length, overburden pressure and degree of saturation of the soil on the pull-out force of GFRP nail

The Pareto chart of standardized effects is plotted in Figure 12. The significant factorial effects are drawn in a down-ranking order and their interaction is identified accordingly. Hence, the overburden pressure, the nail diameter, and the embedded length in addition to their interactions are more statistically significant than the degree of soil saturation in influencing the pull-out force of the GFRP nail.

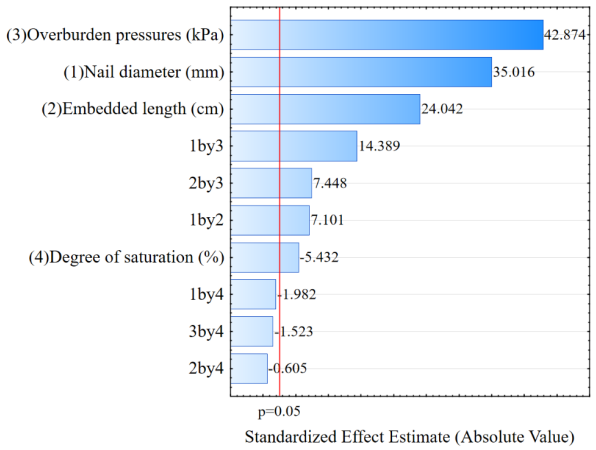

Figure 12 Pareto chart of standardized effects

The measured values served to calculate the regression equations, describing the pull-out force of the GFRP nail. The linear trend and the two-factor interaction coefficients translating the observed behaviours are displayed in Table 6. These results show that the linear model can fairly describe the pull-out force expressed in kN as a function of the nail diameter, the embedded length, and the overburden pressure whilst, the other coefficients are considered negligible. Equation (10) is adopted to describe the linear function of the pull-out force that depends on the three main factors nail diameter, embedded length and the overburden pressure.

$$F = 1.123 + 0.315\,D + 0.216\,L + 0.385\,P \quad (10)$$

Table 6 Effects and interactions of the studied factors

	Effects and interactions
a_0 (Constant term)	1.123
a_1 (Nail diameter)	0.315
a_2 (Embedded length)	0.216
a_3 (Overburden pressure)	0.385
a_4 (Degree of saturation)	-0.049
a_{12}	0.064
a_{13}	0.129
a_{14}	-0.018
a_{23}	0.067
a_{24}	-0.005
a_{34}	-0.014

Figure 13 presents the predicted pull-out force constant contour plot as a function of the nail diameter and the embedded length (Figure 13a), the nail diameter and the overburden pressure (Figure 13b), the nail diameter and the degree of saturation (Figure 13c), the embedded length and the overburden pressure (Figure 13d), the degree of saturation and the embedded length (Figure 13e), and the degree of saturation and the overburden pressure (Figure 13f). As expected, the increase in the nail diameter, the embedded length and the overburden pressure enhance the pull-out force of the GFRP nail. Figure 13 also shows that the pull-out force increases with the increase in the degree of the soil saturation. The pull-out force can reach 2kN with 18-19mm nail diameter, 140-160 kPa overburden pressure, 50cm embedded length and 48% degree of saturation. This example highlights that the nail diameter, the embedded length, and the overburden pressure are significant. They optimize the pull-out resistance of the GFRP nail as an alternative of the steel reinforcement.

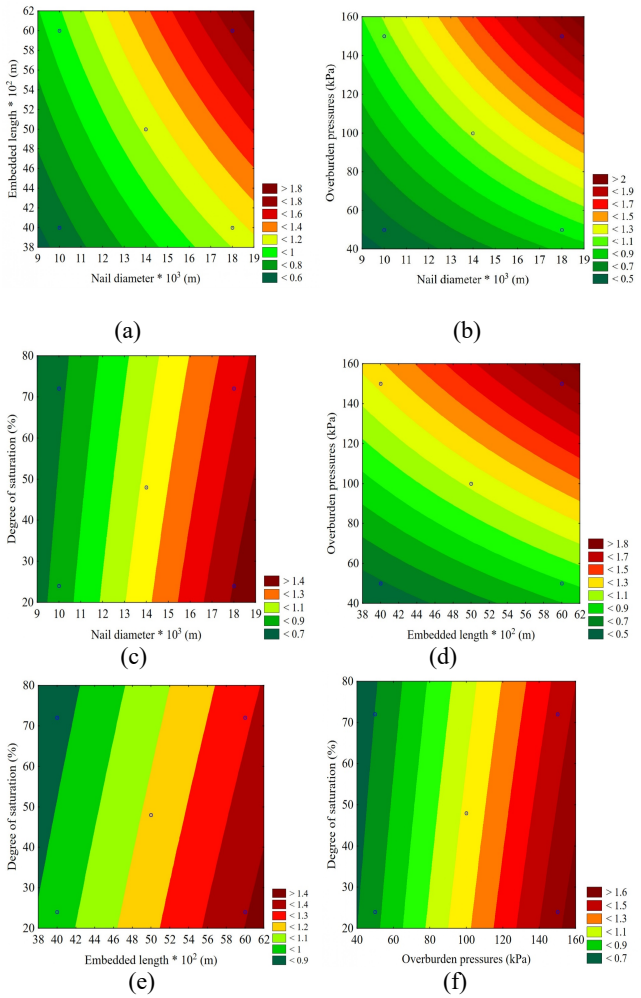

Figure 13 Predicted pull-out force constant contour as function of different factors (a): Y= f (D, L); (b): Y= f (D, OP), (c): Y= f (D, S_r); (d): Y= f (L, OP); (e): Y= f (L, S_r); (f): Y= f (OP , S_r)

4.7 Effect of the Overburden Pressure on the Pull-out Shear Stress of the GFRP Nail

The variation of the peak shear stress τ versus the applied overburden pressure of the GFRP nail tested at 24 % and 72 % degree of saturation are exhibited in Figure 14.

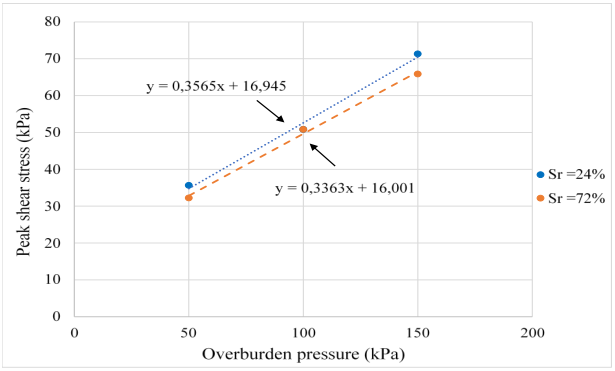

Figure 14 Variation of the peak shear stress τ versus the overburden pressure

The results are in conformity with the pull-out capacity followed by the Mohr-Coulomb failure criterion for the pressure range used in the present study. The increase of the pull-out shear stress in dense soil can be attributed to the restrained dilatancy phenomenon causing an increase in the normal stress locally around the nail. It leads to an increase of the soil density, as well as the normal stress resulting in a higher pullout resistance.

4.8 Effect of the Degree of Saturation of the Soil on the Pull-out Shear Stress of the GFRP Nail

A series of pull-out tests investigated the effect of the degree of the soil saturation on the peak shear stress of the GFRP nail. The tests included two degrees of saturation (24% and 72%). Figure 14 shows that the peak shear stress decreases with an increase of the degree of the soil saturation. However, the decrease remains negligible. Hence, the pull-out capacity of the GFRP nail seems to be insensitive to the soil saturation degree. The equation proposed by Potyondy (1961), based on the Mohr-Coulomb criterion is actually used to correlate the effect of the degree of soil saturation with the interface shear strength of the GFRP nail. In the light of the obtained results, it is noticed that the interface friction angle δ" and the apparent adhesion decrease from 19.62° to 18.59° and from 16.94 kPa to 16 kPa, respectively when the degree of saturation increases from 24% to 72%. These results prove that the degree of saturation does not have a significant influence on the pull-out capacity of the GFRP nail. It can be explained by the property of sand as a draining soil, which is featured by a low water retention capacity.

4.9 Proposed Equations and Engineering Practices

The proposed equations reveal the importance of the failure parameters of the soil-nail's interface, which are essential to characterise the pull-out performance of all types of nails. In fact, the understanding of the soil-nail interface parameters is helpful to solve many pull-out failure problems. Furthermore, the final fitting Equation (10) enables the prediction of the pull-out force of GFRP nails with different diameter, embedded length and overburden pressure ranging from 10mm to 18mm, from 40cm to 50cm and from 50kPa to 150kPa, respectively.

5. CONCLUSIONS AND PERSPECTIVES

A series of laboratory pull-out tests have been performed on the GFRP nail under different conditions to investigate the performance of this new reinforcing material in sand. The test results indicate that the GFRP nail exhibits a pull-out performance different from that of the steel nail. In fact, under the same conditions, the pull-out capacity of the GFRP nail remains lower than that of the steel nail. Furthermore, the pull-out behaviour of the new material is more progressive than that of the conventional one. Such a behaviour is attributable to the geometrical and mechanical properties of these two materials, which are quite different.

The surface roughness of the soil nail seems to have a significant influence on the pull-out behaviour of the ribbed steel and the GFRP nails. The results reveal that with an increase of the related rib area f_r, the peak pull-out resistance will increase under the actual conditions.

A parametric study is established using the full factorial design methodology. It aimed to examine the influence of the factors affecting the pull-out performance of a GFRP nail. It is observed that the pull-out force is governed by the nail diameter, the embedded length, and the overburden pressure. In fact, a larger contact soil nail area and a higher overburden pressure provide a higher GFRP pull-out force. Nevertheless, an increase in the degree of the soil saturation does not have a significant influence on the pull-out behaviour of the GFRP reinforcement since the sand is a draining material.

As a conclusion, the GFRP materials can be an interesting alternative to the steel one for soil nailing.

In the light of the current findings, the following issues may be considered for future studies:

- An investigation of the effect of the soil type on the pull-out capacity of the GFRP nails.
- An investigation of the pull-out capacity of the grouted GFRP nails in sand.

6. ACKNOWLEDGEMENTS

The authors would like to thank Mr. Jan Van Der Perre from Geotechnics laboratory (Faculty of Engineering and Architecture, Ghent University, Belgium) for his considerable contribution in carrying out the sets of experiments.

7. LIST OF NOTATIONS

A	is the active area of the nail
A_n	is the surface of the rib
c'	is the soil cohesion
c_a'	is the soil adhesion at the interface
D	is the nail diameter
F	is the measured pull-out load
f_c	is the coefficient of adhesion
f_Φ	is the coefficient of friction
f_R	is the relative rib area
f_δ	is the interface efficiency ratio
L	is the embedded length
s	is the spacing of the ribs
β	is the angle between the rib and the longitudinal axis of the reinforcement
Φ	is the external diameter of the bar
δ"	is the interface friction angle
Φ'	is the soil internal friction angle
σ	is the initial normal stress acting on the soil nail?
τ	is the ultimate shear stress
RA	is the relative area

7. REFERENCES

Avirut, C., Rottana, S., Suksun, H., Arul, A., and Menglim, H. (2022). "Landslide Rainfull Threshold for Landslide Warning in Northern Thailand." *Geomatics, Natural Hazards and Risk Journal,* 2425-2441, https://doi.org/10.1080/19475705.2022.2120833.

Cheng, Y. M., Au, S. K., and Yeung, A. T. (2016). "Laboratory and Field Evaluation of Several Types of Soil Nails for Different Geological Conditions." *Canadian Geotechnical Journal,* 53(4), 634–645, doi:10.1139/cgj-2015-0267.

Cheng, Y. M., Choi, Y. K., Yeung, A. T., Tham, L. G., Au, A. S., Wei, W. B., and Chen, J. (2009). "New Soil Nail Material-Pilot Study of Grouted GFRP Pipe Nails in Korea and Hong Kong." *Journal of Materials in Civil Engineering,* DOI: 10.1061/(AS CE)0899-1561(2009)21:3 (93).

Chen, Z., Que, M., Zheng, L., Li, X., and Sun, Y. (2020). "Effect of Mortar Constraint Conditions on Pullout Behavior of GFRP Soil Nails." *Advances in Materials Science and Engineering,* doi :10. 1155/2020/4170363.

Chen, Z., Zheng, L., Jin, Q., and Li, X. (2015). "Durability Study on Glass Fiber Reinforced Polymer Soil Nail via Accelerated Aging Test and Long-Term Field Test." *Polymer Composites Journal,* doi: 10.1002/pc.23888.

Correia, S. L., Partala, T., Loch, F. C., Segadães, A. M. (2010). "Factorial Design Used to Model the Compressive Strength of Mortars Containing Recycled Rubber." *Composite Structures,* https://doi.org/10.1016/j. compstruct.2009.11.007.

Hong, Y.S., Wu, C. S., and Yang, S. H. (2003). "Pull-out Resistance of Single and Double Nails in a Model Sandbox." *Canadian Geotechnical Journal,* 1039–1047, doi:10.1139/T03-048.

Junaideen, S. M., Tham, L. G., Law, K. T., Lee, C. F., and Yue, Z. Q. (2004). "Laboratory Study of Soil–Nail Interaction in Loose,

Completely Decomposed Granite." *Canadian Geotechnical Journal,* 274–286, doi:10.1139/T03-094.

Kanoun, F., Haffoudhi, S., Bouassida, M. (2017). "Design and Follow up of 20 m Depth Nailed Wall". *Proceedings of the 19th International Conference on Soil Mechanics and Geotechnical Engineering, Seoul 2017.*

Koor, N., and Cheung, A. (2005). "Double Corrosion Protection of Long Soil Nails at Deep Bay Link–A Case History." *The HKIE Geotechnical Division 25th Annual Seminar: Safe and Green Slopes.*

Lee, C. F., Law, K. T., Tham, L. G., Yue, Z. Q., Junaideen, S. M. (2001). "Design of a Large Soil Box for Studying Soil-nail Interaction in Loose Fill." *Soft Soil Engineering: Proceedings of the Third International Conference on Soft Soil Engineering, Hong Kong:* 413−418.

Linh Van, H. B., Pitcha, J., Bounchi, S., Suched, L. (2022). "Numerical Modelling of Bond Mechanism of ETS FRP Bar–Concrete Joints with Long Embedment Length." *International Journal of Adhesion and Adhesives,* Vol. 117, Part A, September 2022, Article no. 103179, doi: 10.1016/j.ijadhadh.2022.103179.

Mukharjee, B. B., Barai, S. V. (2014). "Statistical Techniques to Analyze Properties of Nanoengineered Concrete Using Recycled Coarse Aggregates." *J. Clean. Prod.* 83, 273–285, https://doi.org/10.1016/j.jclepro.2014.07.045.

Myers, R. H., Montgomery, D. C. (2002). "Response Surface Methodology: Process and Product Optimization Using Designed Experiments." *John Wiley and Sons.*

Nguyen Thanh, Likitlersuang Suched, Ohtsu Hiroyasu, Kitaoka Takafumi (2017). "Influence of the Spatial Variability of Shear Strength Parameters on Rainfall Induced Landslides: A Case Study of Sandstone Slope in Japan." *Arabian Journal of Geosciences,* 10 (16), Article 369, 1 – 12, doi:10.1007/s12517-017-3158-y

Pei, H., Yin, J., Zhu, H., and Hong, C. (2013). "Performance Monitoring of a Glass Fiber-Reinforced Polymer Bar Soil Nail during Laboratory Pullout Test Using FBG Sensing Technology'." *International Journal of Geomechanics,* 13(4), 467–472, doi:10.1061/(asce)gm.1943-5622.0000226.

Pitchaya, O, Apiniti, J, Suched, L. (2022). "Geotechnical Investigation and Stability Analysis of Bio-engineered Slope at Surat Thani Province in Southern Thailand." *Bulletin of Engineering Geology and the Environment,* Vol. 81, Article no. 84, doi:10.1007/s10064-022-02591-5.

Potyondy, J. G. (1961). "Skin Friction between Various Soils and Construction Materials." *Géotechnique,* 11(4), 339–353.

Pradhan, B., Tham, L. G., Yue, Z. Q., Junaideen, S. M., and Lee, C. F. (2006). "Soil – Nail Pullout Interaction in Loose Fill Materials." *International Journal of Geomechanics,* 238–247, doi: 10.1061/ (ASCE)1532-3641(2006)6:4(238).

Samanta, M., Punetha, P., and Sharma, M. (2018). "Influence of Surface Texture on Sand-Steel Interface Strength Response." *Geotechnique Letters,* 8(1),40–48, https://doi.org/10.1680/jgele.17.00135.

Sharma, M., Samanta, M., and Punetha, P. (2019). "Experimental Investigation and Modeling of Pullout Response of Soil Nails in Cohesionless Medium." *International Journal of Geomechanics,* 1–16, doi:10.1061/(ASCE)GM.1943-5622.0001372.

Sharma, M., Samanta, M., and Sarkar, S. (2020). "A Study on Interface Shear Behavior of Soil Nails from Pullout and Direct Shear Tests." *International Journal of Physical Modelling in Geotechnics,* doi:10.1680/jphmg.18.00031.

Shiu, Y. K., and Cheung, W. M. (2003). "Long-term Durability of Steel Soil Nails." *GEO report No.135.*

Shiu, Y. K., and Cheung, W. M. (2014). "Long-term Durability of Steel Soil Nails in Hong Kong." *HKIE Transactions Hong Kong Institution of Engineers,* 15(3), 24–32, doi:10.1080/1023697X.2008.10668121.

Su, L. J., Chan, C. F., Shiu, Y. K., Cheung, T., and Yin, J. H. (2008). "Influence of Degree of Saturation on Soil Nail Pullout Resistance in Compacted Completely Decomposed Granite Fill." *Canadian Geotechnical Journal,* doi:10.1139/T07-056.

Tidarut, J., Tamon, U., Suched, L., Dwei, Z., Nat, H., Nattamet, W., Krittapon, H. (2019). "Effect of Natural Fibre Reinforced Polymers on Confined Compressive Strength of Concrete." *Construction and Building Materials,* Vol. 223, 30 October 2019, 156-164, doi: 10.1016/j.conbuildmat.2019.06.217.

Tidarut, J., Suched, L., Nattamet, W., Tamon, U., Dawei, Z., Marin, S. (2020). "Structural Behavior of Pre-damaged Reinforced Concrete Beams Strengthened with Natural Fibre Reinforced Polymer Composites." *Composite Structures,* Vol. 244, Article No.112309, doi: 10.1016/j.compstruct.2020.112309.

Tidarut, J., Haruna, M., Suched, L., Tamon, U., Jian-Guo, D., Nattamet, W., Nattapong, K. (2021). "Use of Water Hyacinth Waste to Produce Fibre-reinforced Polymer Composites for Concrete Confinement: Mechanical Performance and Environmental Assessment." *Journal of Cleaner Production,* Vol. 292, 10 April 2021, Article no. 126041, doi: 10.1016/j.jclepro.2021.126041.

Tidarut, J., Suched ,L., Nattamet, W., Viganda, V., Wanchai, Y., and Tamon, U. (2021). "Fibre-Reinforced Polymer Made from Plastic Straw for Concrete Confinement: An Alternative Method of Managing Plastic Waste From the COVID-19 Pandemic." *Engineering Journal,* Vol. 53, No. 3, 1-14, doi:10.4186/ej.2021.25.3.1.

Thanh Son, N., Suched, L., Apiniti, J. (2018). "Influence of the Spatial Variability of the Root Cohesion on a Slope-Scale Stability Model: A Case Study of Residual Soil Slope in Thailand." *Bulletin of Engineering Geology and the Environment,* Vol. 78, No. 5,3337-3351, doi:10.1007/s10064-018 -1380-9.

Thanh Son, N., Suched, L., Apiniti, J. (2018). "Stability Analysis of Vegetated Residual Soil Slope in Thailand under Rainfall Conditions." *Environmental Geotechnics,* Vol. 7, no. 5, 338–349, doi:10.1680/jenge.17.00025.

Veerayut Komolvilas, Weeradetch Tanapalungkorn, Panon Latcharote, Suched Likitlersuang (2021). "Failure Analysis on a Heavy Rainfall-Induced Landslide in Huay Khab Mountain in Northern Thailand." *Journal of Mountain Science,* Vol. 18, no. 10, 2580–2596, doi:10.1007/s11629-021-6720-8.

Xu, D. S., Liua, H. B., and Luo, W. L. (2017). "Evaluation of Interface Shear Behavior of GFRP Soil Nails with a Strain Transfer Model and Distributed Fiber-optic Sensors." *Computers and Geotechnics 95,* doi :10.1016/j.compgeo.2017.10.005.

Yeung, A. T., Cheng, Y. M., Tham, L. G., Au, A. S., So, S. T., and Choi, Y. K. (2007). "Field Evaluation of a Glass-Fiber Soil Reinforcement System." *Journal of Performance of Constructed Facilities, 21(1),* doi:10.1061/(ASCE)0887-3828(2007)21:1(26).

Zhang, C. C., Zhu, H. H., Shi, B., Wu, F. D., and Yin, J. H. (2014). "Experimental Investigation of Pullout Behavior of Fiber-Reinforced Polymer Reinforcements in Sand." *Journal of Composites for Construction,* 19(3):04014062, 1–11, doi:10.1061/(ASCE)CC, doi:10.1061/(ASCE)CC.1943-5614.0000526.

Zhang, C. C., Zhu, H. H., Xu, Q., Shi, B., and Mei, G. X. (2015). "Time-Dependent Pullout Behavior of Glass Fiber Reinforced Polymer (GFRP) Soil Nail in Sand." *Canadian Geotechnical Journal,* 52(6), 671– 681, doi :10.1139/cgj-2013-0381.

Zhu, H. H., Yin, J. H., Yeung, A. T., and Jin, W. (2011). "Field Pullout Testing and Performance Evaluation of GFRP Soil Nails." *Journal of Geotechnical and Geo-environmental Engineering,* 137(7), 633–642, doi:10.1061/(asce)gt.1943-5606.0000457.